DNA Adducts of Decarbamoyl Mitomycin C Efficiently Kill Cells without Wild-Type p53 Resulting from Proteasome-Mediated Degradation of Checkpoint Protein 1

Ernest K. Boamah,[†,‖] Angelika Brekman,[†] Maria Tomasz,[‡] Natura Myeku,[†]
Maria Figueiredo-Pereira,[†] Senyene Hunter,[§] Joel Meyer,[§] Rahul C. Bhosle,[†] and
Jill Bargonetti*[,†]

Department of Biological Sciences, and Department of Chemistry, Hunter College and The Graduate Center, CUNY, 695 Park Avenue, New York, New York 10065, and Nicholas School of the Environment, Duke University, Durham, North Carolina 27708

The mitomycin derivative 10-decarbamoyl mitomycin C (DMC) more rapidly activates a p53-independent cell death pathway than mitomycin C (MC). We recently documented that an increased proportion of mitosene1-β-adduct formation occurs in human cells treated with DMC in comparison to those treated with MC. Here, we compare the cellular and molecular response of human cancer cells treated with MC and DMC. We find the increase in mitosene 1-β-adduct formation correlates with a condensed nuclear morphology and increased cytotoxicity in human cancer cells with or without p53. DMC caused more DNA damage than MC in the nuclear and mitochondrial genomes. Checkpoint 1 protein (Chk1) was depleted following DMC, and the depletion of Chk1 by DMC was achieved through the ubiquitin proteasome pathway since chemical inhibition of the proteasome protected against Chk1 depletion. Gene silencing of Chk1 by siRNA increased the cytotoxicity of MC. DMC treatment caused a decrease in the level of total ubiquitinated proteins without increasing proteasome activity, suggesting that DMC mediated DNA adducts facilitate signal transduction to a pathway targeting cellular proteins for proteolysis. Thus, the mitosene-1-β stereoisomeric DNA adducts produced by the DMC signal for a p53-independent mode of cell death correlated with reduced nuclear size, persistent DNA damage, increased ubiquitin proteolysis and reduced Chk1 protein.

Introduction

The p53 protein is an important tumor suppressor and is frequently mutated in cancer cells (*1, 2*). DNA damage activates and stabilizes wild-type p53, which results in increased transcription of multiple p53 target genes involved in cell cycle arrest or apoptotic cell death (*3, 4*). It has been estimated that over 50% of all cancers harbor a mutation in the p53 gene, and this interferes with the ability of the protein to effectively induce cell death (*1*). Loss of p53 function has been associated with increased resistance to chemotherapeutic agents (*5*). In addition, loss of p53 or its downstream target, p21, disrupts the G$_1$/S checkpoint in response to DNA damage (*6, 7*). Lack of a G$_1$/S checkpoint causes cells to depend entirely on their intra-S and G$_2$/M checkpoints to ensure genomic integrity (*8*).

The ataxia-telangiectasia and Rad3-related (ATR[1]) and Checkpoint protein 1 (Chk1) pathways regulate genome fidelity

at the G$_2$/M transition and are especially important to cells lacking a functional p53 checkpoint pathway (*9, 10*). The phosphatidylinositol 3-kinase-related kinase ATR, a DNA damage and replication stress response protein, is part of a complex network of checkpoint proteins which are activated in response to deleterious lesions that affect replication fork progression (*9, 11*). In response to DNA interstrand cross-links and other DNA lesions, ATR phosphorylates Chk1 on two critical residues, Ser-317 and Ser-345 (*12, 13*). When activated, Chk1 delays entry into mitosis by phosphorylating and inactivating Cdc25A and Cdc25C, two phosphatases required for cell cycle progression (*14*). DNA damage recognition activities of the Fanconi anemia core complex cooperate with ATR to signal for interstrand cross-link repair and Chk1 phosphorylation (*15−17*). In the absence of Chk1, cells with DNA damage continue through mitosis culminating in cell death by mitotic catastrophe due to the lack of a G$_2$/M checkpoint (*18−20*). Disruption of the Chk1 G$_2$/M checkpoint kinase is a provocative death target, especially for cells with compromised p53 since these cells lack an efficient G$_1$/S checkpoint (*21−24*).

Mitomycin C (MC), a bioreductive DNA alkylating agent, is a well-known antitumor, antibiotic, and chemotherapeutic agent (*25−27*). Within the intracellular compartment, MC is metabolized by reductive enzymes to generate reactive DNA alkylating species and oxygen radicals through redox cycling (*26*). Activated MC alkylates guanine at the N^2-position to form DNA monoadducts and DNA intrastrand and interstrand cross-link adducts (*28*). 10-Decarbamoyl mitomycin C (DMC), a derivative of MC, has also been shown to bind DNA forming

* To whom correspondence should be addressed. E-mail: bargonetti@genectr.hunter.cuny.edu.

† Department of Biological Sciences.

‡ Department of Chemistry, Hunter College and The Graduate Center, CUNY, 695 Park Ave., NY, NY 10065.

§ Duke University.

‖ Current address: Epigenetics and Progenitor Cells Program, Fox Chase Cancer Center, 333 Cottman Ave., R362, Philadelphia, PA 19111.

[1] Abbreviations: ATR, ataxia-telangiectasia and Rad3-related; Chk1, Checkpoint 1; Chk2, Checkpoint 2; ATM, ataxia telangiectasia mutated; MC, mitomycin C; DMC, decarbamoyl mitomycin C; MTT, 3-(4,5-dimethylthiazol-2-yl)-2,5-diphenyltetrazolium bromide; FBS, fetal bovine serum; G418, gentamycin; DAPI, 4′,6-diamidino-2-phenylindole; RT-PCR, reverse transcriptase-polymerase chain reaction; anti-BPDE, anti-7,8-dihydroxy-9,10-epoxy-7,8,9,10-tetrahydrobenzo[*a*]pyrene.

Mitomycin C (MC)   **Decarbamoyl Mitomycin C (DMC)**
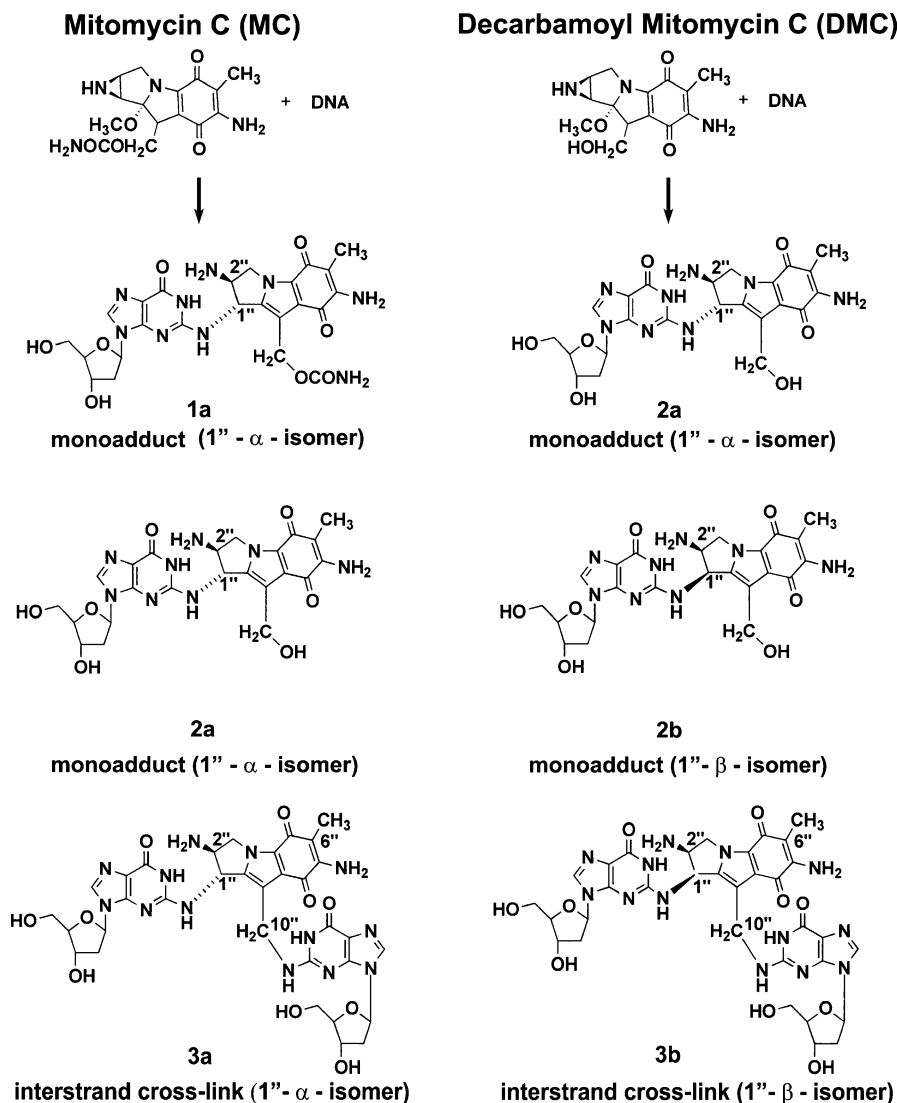
Figure 1. Chemical structures of DNA adducts: **1a**, 1″-α MC monoadduct; **2a**, 1-″α DMC monoadduct; **2b**, 1″-β DMC monoadduct; **3a**, 1″-α interstrand cross-link; **3b**, 1″-β interstrand cross-link.

a similar but not identical array of DNA adducts (*29, 30*). We recently demonstrated that equimolar concentrations of DMC produce more DNA adducts in human cells than MC, and most of the adducts have altered stereochemistry (*30*). Specifically, the chirality of the mitosene linkage of MC to guanine-N² of DNA is opposite of that of DMC (mitosene-1-α vs mitosene-1-β) (Figure 1). The critical cytotoxic lesion produced by chemotherapeutic DNA damaging agents such as mitomycin C has been proposed to be the interstrand cross-link adducts (*31, 32*). These interstrand cross-link DNA modifications, in part, inhibit strand separation during replication and transcription, which in turn activates ATR and ataxia telangiectasia mutated (ATM) checkpoint pathways (*10*). Although both MC and DMC produce these cross-link DNA adducts, interestingly, DMC induces death of cells more rapidly than MC (*29, 33, 34*).

We previously reported that DMC induces the death of many different cell types more rapidly than MC both in the presence and absence of wild-type p53 (*33, 34*). We hypothesized that this difference in cytotoxicity may be based on differential signaling of DNA adducts of MC and DMC. The recent investigation of the nature of the cell death pathways induced by the two drugs suggested that the Chk1 pathway might be involved in differential cytotoxicity (*33*). Moreover, we documented more DNA adduct formation following the treatment

of multiple different types of human cancer cells with DMC than with MC (*30*). The rationale of the present study was to determine whether the mitomycin analogue DMC might be useful for clinical development for cancers that lack wild-type p53 because at equimolar concentrations, DMC is more cytotoxic to p53-deficient cells than MC and thus could be used at lower concentrations to induce cell death. We compared the amount and persistence of the DNA damage induced by the two drugs and compared the cellular and molecular responses of human cancer cells with and without wild-type p53 treated with MC and DMC. We then focused our studies on cells without wild-type p53 (DLD-1) and correlated the DMC induced depletion of the G_2 checkpoint control protein Chk1 with increased cell death and characterized the involvement of the ubiquitin proteolysis pathway in the Chk1 depletion.

Materials and Methods

Caution: *The mitomycins are hazardous chemicals and should be handled carefully.*

Materials. Mitomycin C was obtained from Bristol-Myers Squibb Co., Wallingford, CT and from Kyowa Hakko Kogyo Co. Ltd., Japan. The procedure used for the synthesis of 10-decarbamoyl mitomycin C was as described previously (*35*). Growth medium and penicillin−streptomycin solution were obtained from Mediatech

DNA Adducts Cause Chk1 Depletion by Proteasome

Chem. Res. Toxicol., Vol. 23, No. 7, 2010 **1153**

Inc., Herndon, VA and fetal bovine serum (FBS) and Gentamycin (G418) were purchased from Gemini Bio-Products, West Sacramento, CA. 3-(4,5-Dimethylthiazol-2-yl)-2,5-diphenyltetrazolium bromide (MTT), and MG115 (2-LLnVal) were purchased from Sigma, Allentown, PA. Hygromycin B was purchased from Calbiochem, La Jolla, CA.

Cell Culture, Drugs, and Plasmids. MCF-7 human breast cancer cells (wild-type p53), obtained from American Type Culture Collection, were grown in 90% RPMI/10% fetal bovine serum and penicillin (50 units/mL)−streptomycin (50 μg/mL) solution. The isogenic colon cancer cell lines used were the well characterized DLD-1 and DA-2 lines; they were a generous gift from Bert Vogelstein (Johns Hopkins School of Medicine), whose group used a two-step procedure to establish a tetracycline-off system for controlled wild-type p53 expression in DA-2 cells (*36*). DLD-1 cells do not express wild-type p53, and DA-2 cells maintained in the presence of doxycycline express a trace amount of wild-type p53. DLD-1 cells were grown in 90% McCoys/10% fetal bovine serum and penicillin (50 units/ml)−streptomycin (50 μg/mL) solution, while DA-2 cells were maintained in an additional 0.4 mg/mL G418, 20 ng/mL doxycycline, and 0.25 mg/mL Hygromycin B. All cell culture experiments were carried out at 37 °C in an atmosphere of 95% air/5% CO_2. MC and DMC were dissolved in 30% methanol/70% water. The pCS3$^+$-6Myc plasmid expressing Myc-Chk1 protein was kindly provided by You-Wei Zhang (Salk Institute, La Jolla, CA).

Quantitative PCR-Based Measurement of Nuclear and Mitochondrial DNA Damage. Comparative quantitation of mitochondrial and nuclear genome DNA damage was carried out by quantitative PCR (QPCR) as previously described (*37−39*). Briefly, MCF-7 cells were treated for 1 h with either MC or DMC (10 μM). Following incubation, cells were washed 2× with Hanks buffer and either immediately harvested or allowed to recover in fresh media for 12 h at 37 °C. DNA was isolated from treated and untreated cells and subjected to QPCR for the measurement of nuclear and mitochondrial DNA damage and repair. This assay functions by quantifying the degree of inhibition of PCR amplification observed in damaged samples, compared to control samples, that results from the presence of DNA lesions that block or inhibit the progression of DNA polymerase. Thus, the QPCR assay has the advantage of measuring all polymerase-blocking lesions but the disadvantage of not identifying the nature of the DNA damage. Large portions of the mitochondrial and nuclear genomes were amplified using specific primers. Specifically, primers 2372 and 3927 were used to amplify a 12.2-kb portion of the DNA polymerase β gene, and primers 14841 and 5999 were used to amplify an 8.9-kb portion of the mitochondrial genome, which encompasses roughly 50% of the mitochondrial genome (and thus many genes). Additionally, a small fragment (221 bp) of the mitochondrial genome was amplified using primers 14841 and 14620 (amplifying a small region of the DNA polymerase β gene), and used to monitor the mtDNA copy number as well as to normalize the results obtained from the large mitochondrial fragment. All primer sequences as well as QPCR assay conditions were as indicated by Santos et al. (*38*) Amplifications of treated controls were compared to those of untreated controls to calculate the relative amplification and determine the lesion frequency in treated samples above the basal levels in nontreated controls. Results presented are the mean of at least two sets of PCRs for each amplicon for each sample; $n = 3$ per sample.

Quantitative Reverse Transcription-PCR. RNA was isolated using the Qiagen RNeasy mini kit. Five micrograms of RNA was used for cDNA synthesis using the high capacity cDNA archive kit (Applied Biosystems). The primer-probes for *chk1*, *p21*, and *mdm2* (Applied Biosystems, Celera Discovery Systems Assays on Demand) and *actin* (Applied Biosystems Predeveloped Assay Reagents) were utilized for Taqman PCR using the Applied Biosystems 7500 sequence detection system (Perkin-Elmer) as follows: one cycle, 2 min (50 °C); one cycle, 10 min (94 °C); and 40 cycles, 15 s (94 °C) and 1 min (60 °C).

RNA Interference and Transfections. For siRNA experiments, cells were seeded at 60% confluence in media without penicillin−streptomycin and allowed to attach overnight. Cells were transfected with 25 nM of each of the specified siRNA (all from Dharmacon) for 24 h using Lipofectamine 2000 (Invitrogen). At the end of the incubation period, fresh media without penicillin−streptomycin was added to cells for 2 h, after which cells were either left untreated or treated with 10 μM MC or 10 μM DMC for an additional 24 h. Protein extracts were obtained from cells for Western blot analysis. For 3-(4,5-dimethylthiazol-2-yl)-2,5-diphenyltetrazolium bromide (MTT) analysis, after siRNA transfections, cells were incubated for an additional 2 h with MTT solution and analyzed for proliferation.

For overexpression experiments, cells were plated at 90% confluence and transfected with 4 μg of each indicated plasmid for 24 h using Lipofectamine 2000. Cells were then either left untreated or treated with 10 μM MC or 10 μM DMC for an additional 24 h followed by protein extraction or MTT analysis for proliferation.

Flow Cytometry and MTT analysis. FACS analysis was carried out on a BD Biosciences FACS scan. Cells were washed twice with phosphate-buffered saline (PBS) containing 2% bovine serum albumin and 0.1% NaN_3. Cells were then fixed in 30% ethanol. Propidium iodide staining and RNase treatment were carried out at 37 °C. The viabilities of the cell lines following treatment with DNA damaging agents were determined using the tetrazolium dye-based microtitration assay as described (*33*).

Protein Extract Preparation. Briefly, at the end of the incubation period, cells were harvested, washed 2× in ice-cold PBS at pH 7.5, and spun down after each wash at 300g. Cell pellets were dissolved in RIPA buffer (0.1% w/v SDS, 0.5% w/v deoxycholate, 150 mM NaCl, 1 mM EDTA, 0.5 mM EGTA, 50 mM tris at pH 8.0, 1 mM PMSF, 20 μM aprotinin, and 20 μM leupeptin and supplemented with phosphatase inhibitor cocktail (Sigma) as suggested by the manufacturer) and incubated on ice for 10 min with periodic shaking. Pellets were then centrifuged at 9,300g for 15 min. The supernatants were collected and kept at −80 °C for future analysis.

Western Blot Analysis. Protein samples were size-fractionated by electrophoresis in 10% SDS denaturing poly acrylamide gels and electrotransferred to nitrocellulose membranes (Amersham).

For ubiquitinated products, samples were separated on a 10% and 8% (bottom and top, respectively) denaturing gel prior to transfer. The resulting blots were incubated with the following primary antibodies: p53 specific monoclonal antibodies [1:1:1 mixture of 421, 240, and 1801 antibodies) as described (*40, 41*)], anti-Chk1 (Santa Cruz Biotech., cat. no. sc-7898), antiubiquitin (Dako, cat. no. Z0458), antiproteasome (Biomol, anti-β5 cat. no. PW8895), antimyc (Santa Cruz Biotech., cat. no. sc-40), and the polyclonal antiactin antibody (Sigma). The membranes were then incubated in antimouse or antirabbit secondary antibodies (Sigma), and the signals were visualized by chemiluminescence. Densitometry analysis was performed using NIH imageJ, and values were normalized to actin.

Confocal Microscopy. After drug treatment, cells were fixed with 2% paraformaldehyde in PBS for 15 min at room temperature. Cells were permeabilized with PBS containing 0.2% triton x-100 v/v and 1% fetal bovine serun v/v for 5 min at −20 °C and washed 3× in 1% FBS-PBS. Coverslips were immediately mounted onto slides with 4′, 6′-diamidino-2-phenylindole (DAPI; Vector Laboratories, Inc.). Nuclear morphology was visualized using spinning disk confocal microscopy. All images were captured using a 100× objective. NIH imageJ was used to determine nuclear size.

Proteasome Activity Assay. Native gel proteasome assays were carried out as described previously (*42*). Briefly, cells were washed 2× in PBS and lysed in buffer A (50 mM Tris-HCL pH 7.4, 5 mM $MgCl_2$, 5 mM ATP, 1 mM DTT, and 10% glycerol v/v). Extracts were homogenized on ice and spun down at 4 °C for 15 min at 15,000g. Thirty micrograms of proteins were analyzed on a nondenaturing gradient PAGE gel (5, 4, and 3% from bottom up) with Rhinohide polyacrylamide strengthener (Molecular Probes). Gels were then covered with 0.4 mM of the proteasome substrate,

Table 1. Comparison of the Frequencies of MC- and DMC-Adducts in MCF-7 Cells[a]

drug	1a monoadduct	2a monoadduct	2b monoadduct	3a interstrand cross-link	3b interstrand cross-link
	mol adduct/mol DNA nucleotide ($\times 10^{-7}$)				
MC[b]	1.9	14	1.5	9.3	4.6
DMC[b]		97	148	1.5	27

[a] MCF-7 cells were left untreated or treated for 24 h with 10 μM MC or 10 μM DMC. After treatments, DNA was isolated from the MCF-7 cells and digested to nucleosides. Data represent three independent injections of DNA adducts from the same experiment (*30*). [b] From data in ref *30*; error limits are omitted.

Suc-Leu-Leu-Val-Tyr-AMC (Bachem) diluted in buffer B (buffer A modified to contain 1 mM ATP), and kept at 37 °C for 30 min on a rocker. Proteasome activity bands were visualized when gels were exposed to UV (360 nm). Images were collected using a digital camera.

Results

DMC Caused More Nuclear Shrinkage and DNA Adducts than MC and Generated Persistent Nuclear DNA Damage. We previously reported that DMC has increased cytotoxicity compared to MC in the presence or absence of wild-type p53 with 24 h of drug treatment (*33, 34*) and have shown that the frequency of DNA adduct formation in the MCF-7 wild-type p53 breast cancer cell line is higher for DMC than MC (see Table 1) (*30*). The predominant stereochemistry of the 1″-mitosene linkage of the DMC adducts to DNA was 1″-β (**2b** and **3b**), opposite to the predominant 1″-α stereochemistry of the MC adducts (**1a**, **2a**, and **3a**) (Figure 1 and Table 1). The morphology of MCF-7 cells treated with MC for 24 h showed a barely detectable change in nuclear size as compared to the untreated cells (Figure 2A and B, MCF-7). However, the MCF-7 cells treated with DMC showed a reproducible and statistically significant reduction in size as compared to the untreated population.

To assess if the variable outcome of MC and DMC treatment of MCF-7 cells was cell type specific and if it occurred in the absence of wild-type p53, we compared the nuclear morphology of isogenic colon cancer cells with or without wild-type p53 (DA-2 and DLD-1, respectively) treated with the two drugs (Figure 2A and B). Analysis of nuclear size as compared to the untreated cell population supported the hypothesis that DMC worked through different mechanisms of action than MC, although the different cell types demonstrated variability in their nuclear phenotypes following drug treatment. The nuclear morphology of DA-2 cells treated with MC for 24 h showed a slight increase in size as compared to the same cells that were not treated with the drug (Figure 2A and B, DA-2). However, following 24 h of DMC treatment, DA-2 cells showed a reproducible and statistically significant reduction in their nuclear size as compared to their untreated counterpart (Figure 2A and B, DA-2). In the DLD-1 cells that have no functional p53, MC treatment caused a reproducible and statistically significant increase in nuclear size, while DMC treatment caused a reproducible and statistically significant reduction in the nuclear size. Nuclear shrinkage is often correlated with apoptosis, while swelling is associated with necrosis (*43*).

We also tested whether the variable outcome of DMC vs MC in affecting nuclear morphology correlated with a similar greater potency of DMC to induce damage in the nuclear genome as well as in the mitochondrial genome in the MCF-7 cell line (Figure 3A and B). More DNA damage was caused by DMC than MC to both the mitochondrial genome and the nuclear genome of MCF-7 cells treated with the drugs for 1 h (Figure 3A and B). Furthermore, the most detectable DMC induced mitochondrial DNA damage was removed following 12 h without the drug (Figure 3A), but nuclear DNA adducts caused by DMC persisted 12 h after drug removal (Figure 3B). These results do not indicate that MC caused no DNA damage but rather that under conditions in which DMC caused significant and persistent DNA damage, MC caused no *detectable* damage. The detection limit of this assay is approximately 1 lesion per 10^5 bases (*38*).

Chk1 Depletion Following DMC Treatment Can Be Rescued by Inhibition of the Proteasome. We were specifically interested in the p53-independent mechanism of cell death induced by DMC and for this reason focused on the DLD-1 cell line for the Chk1 studies. The DLD-1 cell line does not contain a functional p53 protein. DMC treatment results in the depletion of Chk1 protein, while MC treatment does not (*33*). To determine if the previously identified Chk1 down-regulation was mediated through a p53-independent ubiquitin−proteasome pathway, we exposed DLD-1 cells to proteasome inhibitors. Total ubiquitinated protein products increased when cells were treated with MG115 (Z-LLnVal) (Figure 4A, compare lanes 1 and 2) or with MG132 (Z-LLLal, data not shown). As expected, DMC, but not MC, treatment caused the depletion of Chk1 protein (Figure 4A, lanes 3 and 5). However, unexpectedly, the total ubiquitinated proteins also decreased. Importantly, Chk1 levels and total ubiquitinated proteins were recovered in the presence of MG115 (Figure 4A, compare lanes 5 and 6). The recovery of Chk1 upon successful inhibition of the proteasome pathway implicates the proteasome as the primary mechanism for Chk1 degradation in DMC treated cells (Figure 4A, lanes 5 and 6). This mechanism of Chk1 regulation in DMC treated DLD-1 cells, which do not express wild-type p53, was also observed in DA-2 cells which express wild-type p53 (data not shown).

DMC DNA Adducts Activate Signaling for Protein Degradation without Increasing Proteasome Activity. While Chk1 depletion was clearly facilitated by the ubiquititin proteosome pathway, we had not determined the signaling mechanism associated with its down-regulation. In our current investigation, we observed concomitant depletion of total ubiquitinated protein (Figure 4A, lane 5). Increased degradation of total ubiquitinated protein suggested that perhaps DNA adducts of DMC signaled for an increase in proteasome activity. We used an established in-gel assay to detect, in cell lysates, the cleavage of the fluorogenic peptide substrate Suc-Leu-Leu-Val-Tyr-AMC, by the proteasome core particle with both regulatory particles (RP$_2$CP), core particle with one regulatory particle (RP$_1$CP), and only the core particle (CP) (*42*). The inhibitor, MG115 decreased proteasome activity in DLD-1 cells (without wild-type p53) (Figure 4B, left panel, lane 2). However, MC and DMC treatment did not increase proteasome activity compared to that in the untreated samples (Figure 4B, compare lanes 3 and 4 to lane 1). The increased degradation of ubiquitinated substrates in DMC treated cells was not due to a change in proteasome levels or proteasome activity since DMC treated and untreated cells showed similar proteasome levels and activity, respectively (Figure 4B, compare the left panel to the right panel). The observed decrease in ubiquitinated products in the absence of an increase in proteasome activity suggested that DNA adducts of DMC might increase signaling to the proteolysis machinery.
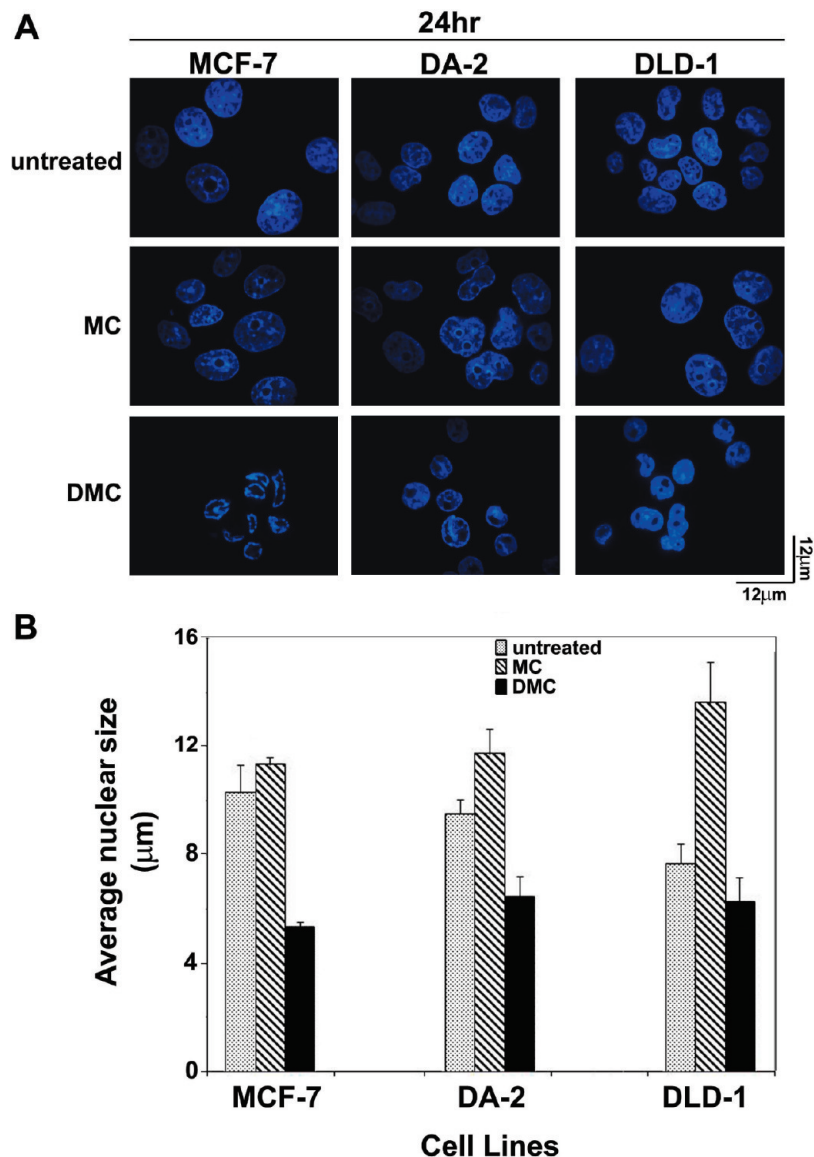
Figure 2. DMC cytotoxicity is associated with decrease in nuclear size. MCF-7, DA-2, and DLD-1 cells were left untreated or treated for 24 h with 10 μM MC or 10 μM DMC. (A) Representative region of the DAPI stained slide with nuclei from 3 independent experiments is depicted. (B) Nuclei sizes were determined after staining cells grown on a coverslip with DAPI. Average values obtained from 2 independent experiments are calculated. For each independent experiment, the number of nuclei measured for each treatment condition was MCF-7 (*29*); DA-2 (*32*); and DLD-1 (*21*). Error bars denote SEM, and the significance was determined using a one-tailed paired *t* test for the drug treated samples compared to the untreated controls. *P*-values of 0.05 or less resulted for DA-2 cells treated with DMC; *P*-value = 0.03; DLD-1 cells treated with DMC, *P*-value = 0.05; and DLD-1 cells treated with MC, *P*-value = 0.05. *P*-value = paired *t* test.

To determine if the rescue of Chk1 protein levels by MG115 was due to protein stabilization and not an increase in *chk1* RNA, we examined the levels of total *chk1* mRNA before and after the inhibition of the proteasome (Figure 4C). MG115 treatment did not significantly change the levels of the *chk1* transcript under any of the test conditions (Figure 4C). DMC treatment resulted in the reduction of total *chk1* mRNA; however, the rescue in Chk1 protein accumulation seen in Figure 4A was clearly due to a change in Chk1 stability and not mRNA level as the *chk1* mRNA level was not increased upon MG115 treatment.

The chemical composition of the two mitomycin agents is similar enough that variable toxicity to human cells at equimolar concentrations, in combination with our previous adduct structure data, suggests that the two drugs possess different modes of action. However, comparing equimolar versus equitoxic doses is also important for addressing the question of different pathways of activation. Because of the high toxicity of DMC,

it was not simple to achieve equal cytotoxicity to MC. We determined that decreasing the concentration of DMC by 10-fold resulted in cytotoxicity comparable to that seen with MC, resulting in sufficient live cells to examine the biology (Figure 4D). When concentrations of 1 μM to 50 μM of the two agents were compared for the p53-deficient cells, the cell morphology and MTT data indicated a similar cytotoxicity of the two drugs at 1 μM DMC and 10 μM MC (Figure 4D and D′). At these comparable concentrations, the p53-deficient cells were equally alive as indicated by mitochondrial activity and matrix attachment. We then asked, how does the signaling of the two agents compare at these concentrations when very few cells were dead? Classification of checkpoint pathways is nontrivial, and the methods used to characterize the cellular changes must be superimposed on the drug treatment itself. We examined the cell cycle distribution of the p53-deficient cells as an indicator of how the two agents influenced the cell cycle populations when the cells showed similar mitochondrial activity. We found a

A

B
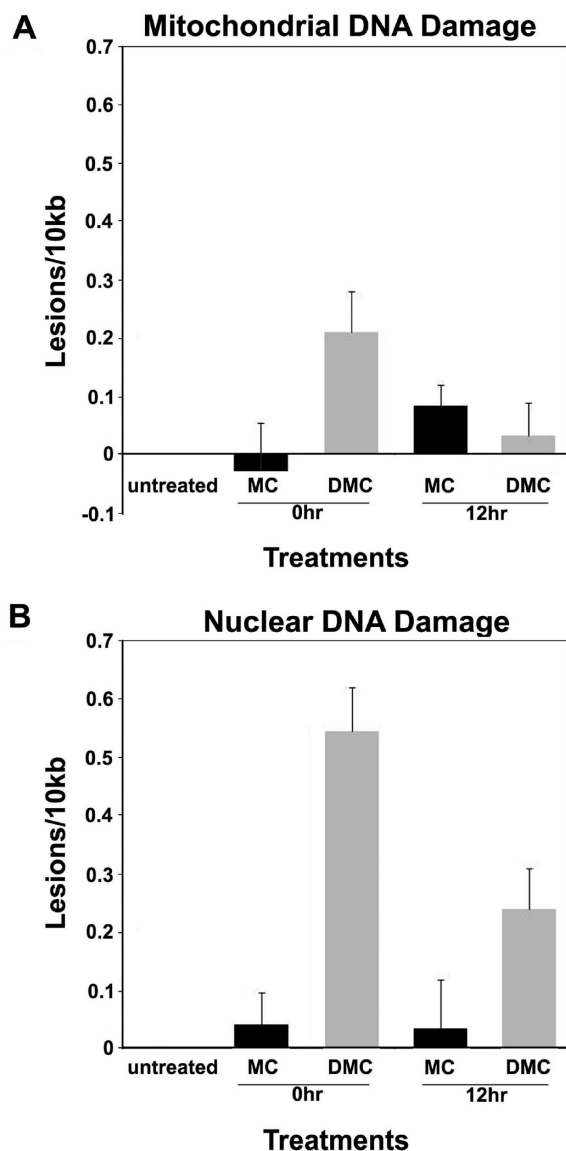
Figure 3. DMC induces more mitochondrial and nuclear DNA damage than MC. Nuclear and mitochondrial DNA damage was assessed by QPCR. MCF-7 cells were treated with MC or DMC (10 μM). Cells were either harvested immediately after treatment (0 h) or allowed to recover for 12 h. Isolated DNA was subjected to QPCR, and the amplification of each treated sample was compared to untreated controls to determine the relative amplification. These values were then used to calculate the average number of lesions obtained per 10kb of the genome. Error bars indicate the SEM for triplicate samples.

striking difference in the cell cycle profiles with the two drugs at equitoxic concentrations (Figure 4D''). The p53-deficient cells treated with 1 μM DMC piled up in the S and G2/M stages, while the 10 μM MC treated cells were found mostly in G1 (Figure 4D'' FACS). We also examined the Chk1 protein level in these treated cell populations and found that Chk1 was not reduced during this early differential cell cycle response (Figure 4E). When the cells were equally alive, the Chk1 levels were similar, but the cell cycle distribution was very different, suggesting that a different signaling pathway was engaged. Our hypothesis is that MC and DMC can mechanistically influence p53-deficient human cells in different ways and that Chk1 depletion is a later stage event that correlates with cell death.

Depletion of Chk1 by siRNA Increased MC Cytotoxicity, while Overexpression of Chk1 Slightly Attenuated DMC Induced Cell Death in the Absence of Wild-Type p53. Since we observed differential regulation of Chk1 during MC- and

DMC- induced cellular cytotoxicity, we hypothesized that the Chk1 protein might play a role in the differential cytotoxicity observed for the two drugs. To address this hypothesis, we depleted the levels of endogenous Chk1 using siRNA and observed the outcome of drug treatment (Figure 5A, see lanes 7−9). In the absence of Chk1 siRNA, down-regulation of Chk1 protein was only seen in DMC treated cells (Figure 5A, see lanes 3 and 6). In the presence of Chk1 siRNA, we observed the dramatic reduction of Chk1 protein in MC treated cells and investigated if this, as predicted, increased the cytotoxicity of MC (Figure 5A see lanes 7−9). We observed a statistically significant decrease in cell proliferation in MC treated samples when Chk1 was depleted by Chk1 siRNA (Figure 5B, comparing nonspecific siRNA to Chk1-siRNA). Cells that had been treated with MC showed the most significant decrease in percent viable cells with siRNA to Chk1 as compared to the nonspecific siRNA (Figure 5B). Moreover, the cellular cytotoxicity of MC was not changed when cells were treated with Mdm2 siRNA used as an unrelated target control. As predicted, Chk1 depletion increased MC induced death suggesting that any conditions that reduce the amount of Chk1 also reduce cell viability. The fact that DMC treatment reduces Chk1, before the addition of Chk1 siRNA, renders the siRNA addition here less significant.

To address the potential of stabilized Chk1 to attenuate DMC cytotoxicity, we overexpressed a Myc-tagged Chk1 protein, which was successfully induced under all treatment conditions (Figure 5C). However, only the endogenous Chk1 protein was selectively down-regulated by DMC, while the exogenous Myc-Chk1 protein was not (Figure 5C, lane 6). The Myc-tagged Chk1 protein used in our experiments has been reported to induce phosphorylation of its downstream target Cdc25C *in vitro*, but this exogenous Chk1 has been shown to be less sensitive to ATR mediated phosphorylation, activation, and proteasome mediated degradation (*44*). Treatment with MC did not dramatically influence either endogenous or exogenous Chk1 (Figure 5C, compare lanes 2 and 4). We examined the role of stabilized Myc-Chk1 in mitomycin induced cellular cytotoxicity (Figure 5C, graph). When exogenous Chk1 was introduced, viability increased only slightly above the vector control (Figure 5C, graph). The limited rescue observed may be explained by the decreased activation for this exogenous Chk1 by the ATR mediated phosphorylation documented previously. However, the slight increase in viability observed with the addition of exogenous Chk1 might be explained by a limited increase in activation of the G2/M checkpoint.

DMC DNA Adducts Interfere with p53 Transcriptional Activity. While our studies have focused on the p53-independent activity of MC and DMC in DLD-1 cells, the possibility existed that the persistent nuclear DNA damage for 24 h with DMC might influence wild-type p53 mediated activation of transcription differently than MC. Therefore, the outcome of 24 h treatment with MC and DMC on DNA damage induced transcriptional activity of wild-type p53 was assessed in the p53-proficient MCF-7 cells and DA-2 cells. Both MC and DMC treatment stabilized p53 in both cell lines as determined by Western blot analysis (Figure 6A and B). The stabilized wild-type p53 after 24 h of 10 μM treatment with MC robustly activated transcription of the p53 target genes *mdm2* and *p21*. However, following 24 h of 10 μM DMC treatment, the stabilized p53 resulted in less activation of *p21* than MC and did not result in transactivation of *mdm2* (in fact, a decrease was observed) (Figure 6A and B). The possibility exists that the increased frequency of DNA adducts by DMC or perhaps the mitosene-1-β-DNA adduct stereochemistry produced by
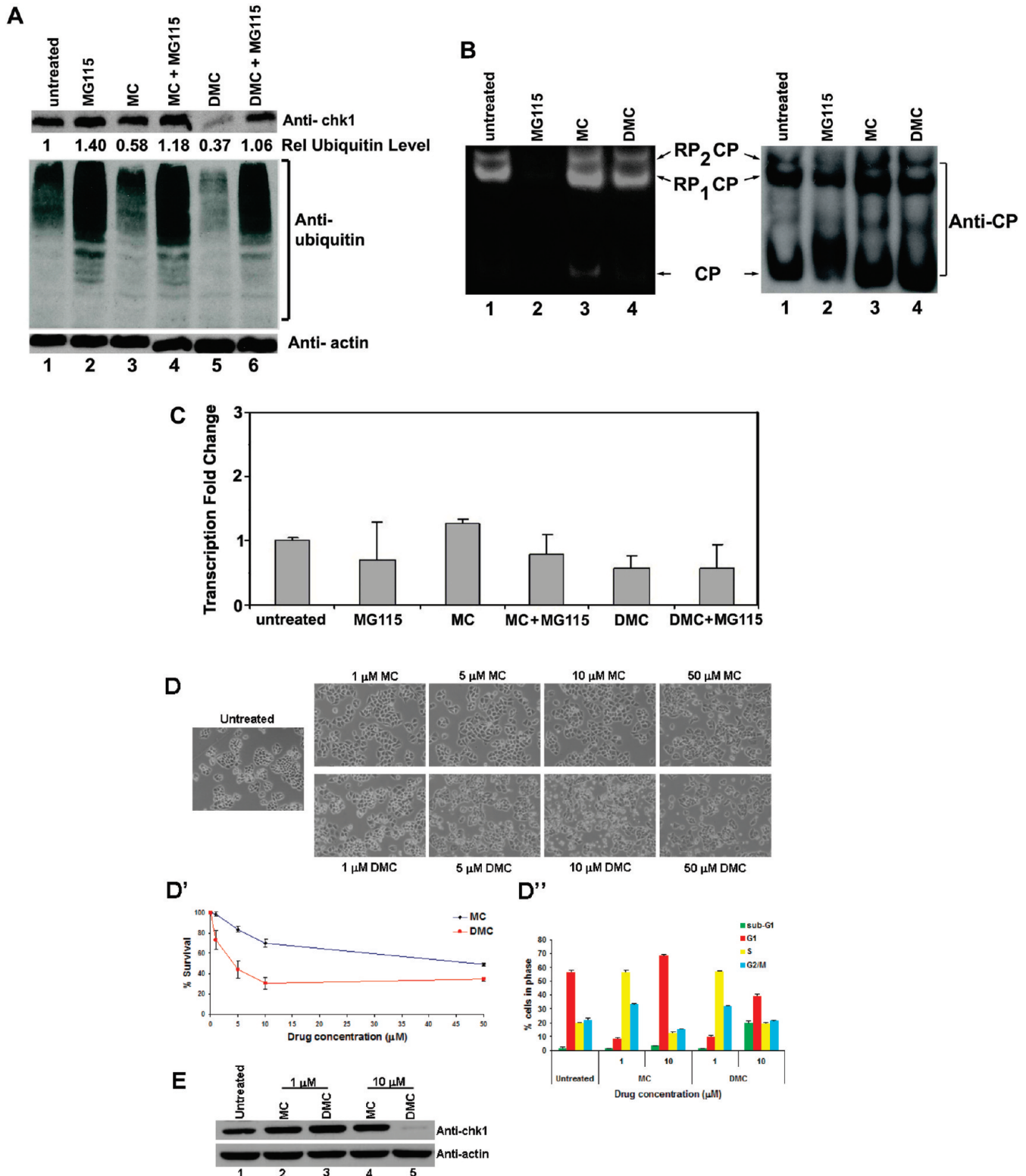
Figure 4. DMC treatment activates a proteasome dependent depletion of Chk1 without increasing proteasome activity. (A) Whole cell extracts obtained from DLD-1 cells were left untreated (lane 1), treated with 4 μM MG115 (lane 2), 10 μM MC or 10 μM DMC (lanes 3 and 5), and 10 μM MC or 10 μM DMC with 4 μM MG115 (lanes 4 and 6), and were analyzed by Western blotting for Chk1 protein (top panels) and accumulation of ubiquitinated proteins (bottom panels). Actin was used as a loading control. Numbers at the top of each sample lane on the ubiquitin blot represent the relative Chk1 protein normalized to actin. (B) Native gel proteasome assay shows no change in proteasome activity. DLD-1 cells were left untreated (lane 1) and treated with 4 μM MG115 (lane 2), 10 μM MC (lane 3), or 10 μM DMC (lane 4). Extracts were obtained from cells and analyzed on a native polyacrylamide gel for proteasome activity (left panel) and Western blot for proteasome subunits (right panel). The different proteasome forms are labeled as RP$_2$CP, RP$_1$CP, or CP. (C) Fold change mRNA levels for *chk1* RNA were analyzed by quantitative real-time reverse transcriptase-polymerase chain reaction PCR (RT-PCR). Results were normalized to untreated samples and *actin* values. Error bars indicate the standard deviations of two independent experiments. (D) Phase contrast image of DLD-1 cells treated with MC and DMC as indicated. (D′) MTT analysis of cells treated with MC or DMC. (D″) FACS analysis of DLD-1 cells treated with either 1 μM or 10 μM of MC or DMC. (E) Whole cell extracts obtained from DLD-1 cells treated with either 1 μM or 10 μM of MC or DMC were analyzed by Western blotting for Chk1 protein. Actin was used as a loading control.

A

B

C
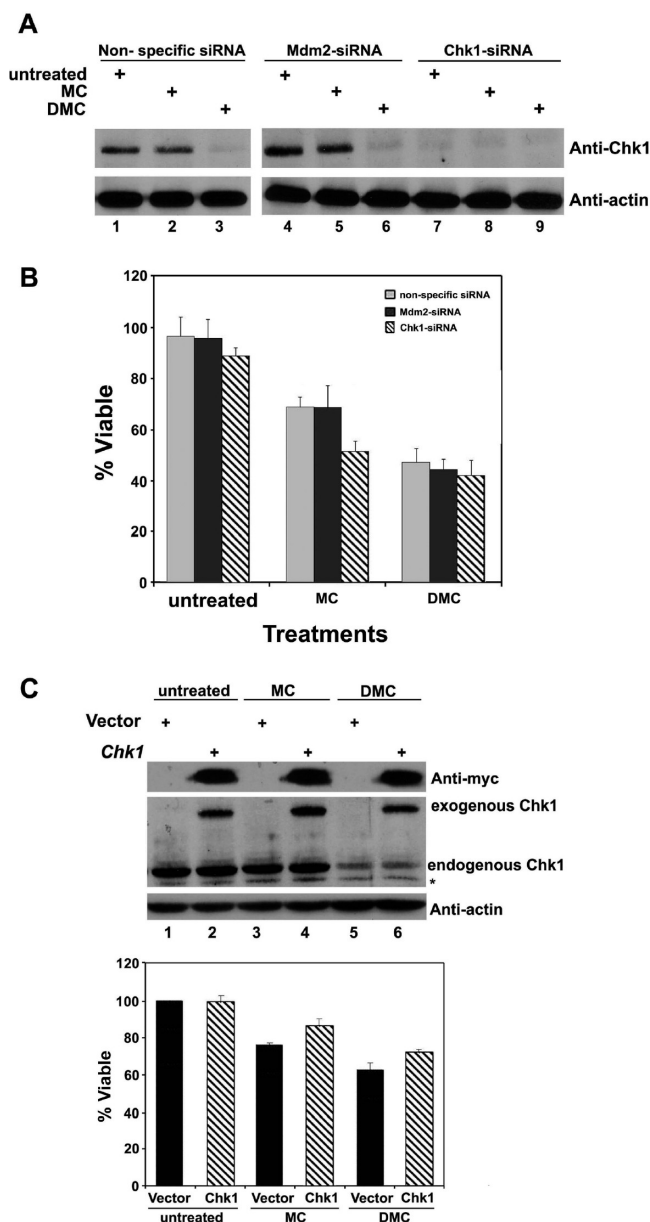
Figure 5. Chk1 down-regulation increased MC cytotoxicity in the absence of wild-type p53. (A) DLD-1 cells were left untransfected or transfected with 25 nM nonspecific siRNA, 25 nM Mdm2 siRNA, or 25 nM Chk1 siRNA for 24 h. After the transfection incubation period, cells were either left untreated or treated with 10 μM MC or 10 μM DMC for an additional 24 h. Whole cell extracts were obtained from these cells and analyzed for Chk1 expression. Actin was used as a loading control. (B) To determine the percent proliferation, cells were treated as indicated above. MTT solution was added to each sample and incubated for an additional 2 h. Values were obtained from 3 independent experiments, and significance was determined for the siRNA treatment as compared to the drug treated control. *P*-values below 0.05 were obtained for all samples treated with siRNA to Chk1. Error bars denote SEM. *P*-value = paired *t* test. (C) For overexpression, cells were transfected with 4 μg of either empty vector or *Myc-Chk1* for 24 h. After the transfection incubation period, cells were either left untreated or treated with 10 μM MC or 10 μM DMC for an additional 24 h. Whole cell extracts were obtained from these cells and analyzed for Chk1 expression. Actin was used as a loading control. To evaluate the proliferation of cells overexpressing *Myc-Chk1* after treatment with MC or DMC, cells were treated as indicated above. MTT solution was added to each sample, and cells were incubated for an additional 2 h. Values were obtained from 3 independent experiments. Error bars denote SEM.

DMC interferes with the ability of the basal transcription machinery to produce transcripts from the *mdm2* gene and reduced transcription from the *p21* gene. We have previously noted that at early time points (3 and 6 h) after 10 μM MC and DMC treatment transcription of the p53 target genes is similar

(*34*); the decrease seen here could also be due to increased induction of cell death after 24 h. Nevertheless, the different outcomes of MC and DMC treatment on p53-proficient cells and on the p53-pathway are another indication that DMC and MC can signal to the cellular machinery differently when used at similar concentrations. When we compared the p53-proficient MCF-7 cells treated with the two drugs at concentrations ranging from 1 μM to 50 μM, a 10-fold difference for the cytotoxic concentration was observed by MTT analysis and visualization of matrix attachment (Figure 6C and C′). Interestingly, while 1 μM DMC treatment was equally cytotoxic to 10 μM MC, the p53 stabilization achieved at the two concentrations was significantly different (Figure 6C″, compare lanes 3 and 4); 10 μM MC resulted in a more robust stabilization of p53 than 1 μM DMC treatment. In addition, the equal p53 response at the 1 μM dose in the p53-proficient cells clearly showed highly different cytotoxicity levels for the two drugs (Figure 6C″, lanes 2 and 3). This is yet another indication that increased cytotoxicity of DMC as compared to MC is through a p53-independent pathway.

Discussion

Down-regulation of Chk1 has been described as an alternative pathway for inducing cell death when the more common apoptotic pathways have been sabotaged in cancer cells (*22, 45*). We observed Chk1 down-regulation and increased cell death, especially in the absence of a p53 checkpoint, when cells were treated with DMC (*33*). Treatment with DMC produces more mitosene-1-β-DNA adducts than MC (*29, 30*). DMC is more cytotoxic than MC (*29*), and this increased cytotoxicity does not depend on the function of wild-type p53, which makes DMC a promising drug for the many cancers that contain mutant p53 (*33, 34*). In view of the close structural similarity between MC and DMC, the differences in their biological effects in human tumor cell cultures were originally unexpected. In this article, we further characterize these effects and propose to correlate them with the known structural differences of the DNA adducts, the amount of adduct formation, and cellular signaling.

Interstrand cross-link (ICL) DNA adducts are the clinically relevant cytotoxic lesions produced upon exposure to MC and DMC (*29*). The intrinsic ability of the cellular machinery to recognize and excise ICL lesions from the genome and activate cell death when genomic integrity is beyond repair underlies the sensitivity of various cell lines to DNA cross-linking (*32*). The increased production of mitosene-1-β-DNA adducts following DMC treatment or their persistence in the nuclear genome might account for the reduction in nuclear size that correlates with the increased cytotoxicity observed with this mitomycin derivative. The nature of the mitosene-1-β interstrand cross-links and how they contribute to cytotoxicity are just beginning to emerge and will provide useful tools for dissecting how different DNA adduct structures signal to alternative cell death pathways. Such information could be useful in the design of compounds to target cancers containing a compromised p53 pathway. Our model for how DMC-damaged DNA signals differently from MC-damaged DNA is presented in Figure 6D.

DMC treatment of cells caused a reduction in nuclear size which is consistent with a number of types of cell death including mitotic catastrophe and apoptosis (*46*), while swelling is associated with necrosis (*43*). The DLD-1 cells do not have functional p53 and showed nuclear shrinkage with DMC treatment and swelling with MC treatment. This difference in morphological outcome when the cells are treated at the same concentration supports the possibility that the structural differ-
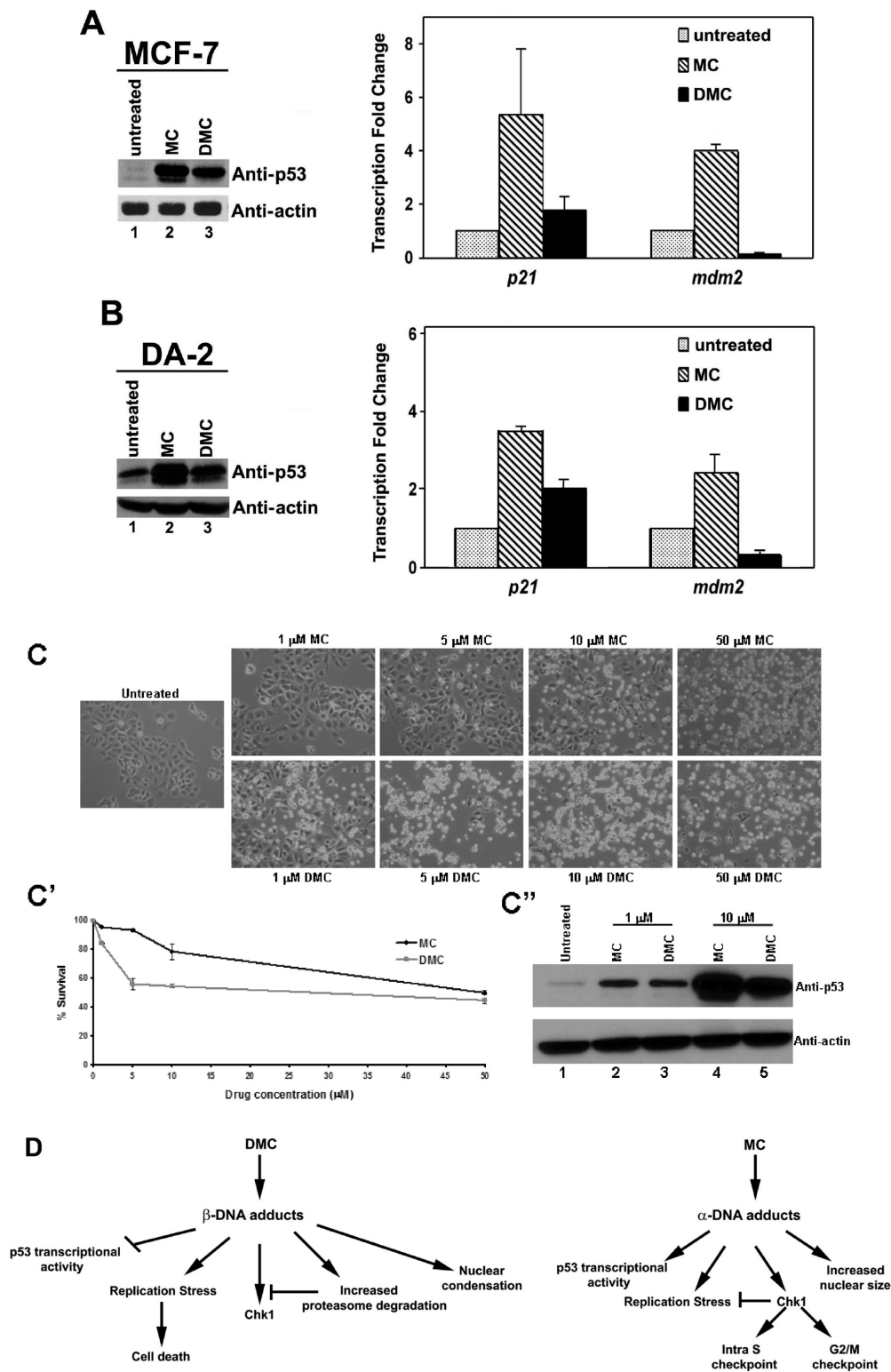
Figure 6. DMC DNA adducts disrupt p53 transcriptional activity. (A) MCF-7 and (B) DA-2 cells were left untreated (lane 1) or treated for 24 h with 10 μM MC (lane 2) or 10 μM DMC (lane 3). After treatments, whole cell extracts were obtained from cells and analyzed for p53 protein stability. Actin was used as a loading control. For quantitative PCR analysis, cells were left untreated or treated for 24 h with 10 μM MC or 10 μM DMC. Transcriptional activity of p53 target genes, *p21* and *mdm2* mRNA, were analyzed by quantitative real-time reverse transcriptase-polymerase chain reaction PCR (RT-PCR). Results were normalized to untreated samples and *actin* values. Error bars indicate the standard deviations of two independent experiments. (C) Phase contrast image of MCF-7 cells treated with MC and DMC as indicated. (C′) MTT analysis of cells treated with MC or DMC. (C″) Whole cell extracts obtained from MCF-7 cells treated with either 1 μM or 10 μM of MC or DMC were analyzed by Western blotting for p53 protein. Actin was used as a loading control. (D) Model:DMC treatment generates increased amounts of the mitosene-1-β DNA adducts, while the MC treatment produces moderate amounts of mitosene-1-α DNA adducts. The increased DNA adducts produced by DMC after 24 h interfere with p53 transcriptional activity, signal for the rapid depletion of endogenous Chk1 by the proteasome, which may disrupt the G$_2$/M cell cycle checkpoint and lead to nuclear condensation. The inability of cells to arrest at the G2/M checkpoint due to the lack of Chk1 potentiates cytotoxicity of DMC. MC DNA adducts activate Chk1, which may prolong the Intra S and G$_2$ checkpoints, increase nuclear size, and activate p53 transcriptional activity, while blocking replication stress induced cell death.

ence of drugs can cause different types of cell death, especially in the absence of p53 function. We documented previously that caspase-3 and -9 activation and PARP cleavage are limited in DMC treated cells lacking p53 (*33*), but we have not examined the activation of caspase-2. An alternative apoptotic program, which requires caspase-2, can be engaged in cells with depleted Chk1, and this pathway is not affected by p53 loss (*47*). Our data demonstrate that Chk1 depletion can increase the extent of MC induced cell death and is correlated with DMC induced cell death; but our data do not indicate if the mechanism is through mitotic catastrophe or a caspase 2-dependent cell death. It should be noted that micronuclei formation has been reported as a characteristic of cells undergoing DNA damage induced mitotic catastrophe (*46, 48*). The possibility of cytokinesis in the absence of complete DNA replication due to increased cross-links and loss of Chk1 dependent checkpoint could account for the observed micronuclei. While we do not have direct evidence for this, our confocal microscopy images of DAPI stained nuclei (Figure 2) show brightly stained condensed nuclear architecture after the cells were treated with DMC for 24 h.

It is known that ICLs disrupt DNA replication and transcription (*32*). ICLs are mostly cytotoxic to cells in the S phase, which are actively replicating, because these aberrant DNA structures inhibit replication by stalling the polymerase. The stalled polymerase activates DNA damage response factors and checkpoint regulators (*10*). The ability of Chk1 to arrest the cell cycle has been shown to prolong cell survival after DNA damage (*49, 50*). It is shown here that increased production of mitosene-1-β-DNA adducts by DMC correlates with a signaling mechanism that results in the down-regulation of Chk1 by the ubiquitin proteolysis pathway. In the absence of Chk1, DNA-damaged cells can continue through the G_2/M checkpoint eventually causing death. Recently, it was reported that ATR/Chk1 signaling is highly specific to replication blockers as opposed to the alternative ATM/Chk2 regulatory pathway (*45, 51*). This suggests that the primary pathway activated by replication blockers to induce recovery from DNA damage and prolong cell survival is through the ATR/Chk1 pathway. The regulation of Chk1 we have observed correlates well with the differential activation of this pathway by MC and DMC. Sporadically, we see that 24 h treatment of cells with MC results in increased Chk1 protein levels; however, we never see a reduction of Chk1 at the 24 h time point (*33*). We previously showed that increasing the time of MC treatment to 72 h caused a reduction in the Chk1 level; here, we show that increasing the MC concentration by 10-fold (to 100 μM) causes a reduction in Chk1. Therefore, when the treatment conditions with MC are pushed to cytotoxic limits we do see a reduction in Chk1 that correlates with cytotoxicity in cells without wild-type p53.

When Chk1 was down-regulated by siRNA, similar cytotoxicity of equimolar MC and DMC was achieved. Consistent with our current data, Sugiyama et al. reported that disruption of the Chk1 G_2 checkpoint using UCN-01, a Chk1 inhibitor, increased the cytotoxicity of MC, and this effect was independent of the wild-type p53 (*52*). However, overexpressing Chk1 caused only a slight decrease in the cytotoxicity of the two mitomycins at 24 h post-treatment. The activity of the exogenous Chk1 is limited, and therefore, the slight increase in viability detected is most likely due to this fact (*44*). It is possibile that the exogenous Chk1 lacked significant kinase activity or that the lack of upstream or downstream factors that influence Chk1 activity were down-regulated by DMC DNA adduct signaling. Down-regulation of these factors might render exogenous Chk1 insufficient to significantly affect the cellular outcome after

overexpression. However, since we observed a slight increase in survival after Chk1 overexpression, it remains possible that overexpressed Chk1 could rescue survival but requires additional factors.

The regulation of Chk1 has been implicated in the response of cells to replication blockers. Phosphorylation of Chk1 by ATR at Ser345 as opposed to Ser317 preferentially destabilizes Chk1 by marking it for ubiquitin mediated proteolysis. Chk1 is now a target for cancer therapy (*12, 53*). We observed that when the proteasome activity was inhibited by MG115, Chk1 protein levels were recovered even when cells were treated with DMC. Our data support the hypothesis that DMC down-regulates Chk1 by causing increased ubiquitination and subsequent degradation by the proteasome. Importantly, we saw that this mechanism of Chk1 down-regulation happened in the absence of increased proteasome activation. We did not observe any increase in proteasome activity in DMC treated samples but observed a decrease in total ubiquitinated protein products upon treatment with DMC. This supports the hypothesis that DMC DNA adducts signal for altered protein post-translational modifications that cause rapid degradation of the tagged polypeptides. This was substantiated by preliminary protein microarray data showing that DMC treatment caused a dramatic reduction in the levels of many proteins on the Sigma Panorama Cell Signaling antibody array (data not shown).

When we examined the p53 transcriptional activity, we observed that while both MC and DMC could stabilize p53, the p53 in 24 h DMC treated cells did not correlate with increased levels of the *mdm2* gene transcript and resulted in lower *p21* transcription than that seen in MC treated cells. Robust activation of both *mdm2* and *p21* was evident in MC treated cells. The reduced p53 transcriptional activity following DMC treatment may be due to the fact that the persistent DNA adducts of DMC, over time, negatively influence the transcription machinery. This suggests that even in the presence of wild-type p53 protein, DMC might activate a parallel p53-independent pathway because the p53 target genes are not as robustly turned on by DMC in spite of stabilization of the p53 protein. Inhibition of *mdm2* transcription by DNA damage is not novel, for example, etoposide induced DNA damage has also been reported to disrupt transcription of the p53 target gene *mdm2* (*54*). The parallel death pathways of p53 activation and p53-independent cell death by DMC will require further investigation.

We observed that DMC induces p53-independent cell death in cancer cells in a manner that correlated with ubiquitin mediated degradation of Chk1 in the presence of persistent DNA damage. We see that Chk1 degradation is correlated with the predominant formation of mitosene-1-β guanine adducts of DMC, in contrast to the mitosene-1-α adducts formed with MC. This alteration of the chirality of the drug linkage to DNA undoubtedly changes the alignment of DMC adducts, and this may be related to the basis of the different DNA damage signaling mechanisms (see model in Figure 6). The alignment of the MC mitosene-1-α monoadduct and of the 1-α cross-link in oligonucleotide duplexes has been well characterized (*55–57*). The alignment of the mitosene 1-β adducts of DMC have not been studied yet.

The mitomycins represent a case in which DNA linkage chirality is proposed to modulate the biological response to DNA damage. Well-studied precedents of a relationship of DNA adduct chirality to biological activity exist, most notably the case of the adducts of racemic anti-7,8-dihydroxy-9,10-epoxy-7,8,9,10-tetrahydrobenzo[*a*]pyrene (anti-BPDE). The highly

tumorigenic (+)-anti-BPDE enantiomer mostly forms (90%) the (+)-*trans*-anti [BP]-N^2-dG adduct, while the nontumorigenic (−)-anti-BPDE enantiomer forms (−)-*trans*-anti- and (−)-*cis*-anti-[BP]-N^2-dG adducts. The latter two adducts are linked to the N^2 atom of dG with chirality opposite to that of the (+)-*trans*-anti-[BP] adduct (*58*).

The available data of the present investigation do not allow us to distinguish with certainty whether the observed differential signaling by MC and DMC is due to the difference in their adduct frequency (*29, 30* see also Table 1) or to intrinsic structural differences of their adducts critical for signaling. It will be necessary to compare these effects at equivalent adduct frequencies. With respect to the first alternative, it is likely that the more intense DNA alkylating activity of DMC compared to that of MC *in vivo* is facilitated by its lack of the 10″-carbamoyl group. This group may hinder the attack by MC, especially of the production of the MC 1″-*β*-dG adducts which are formed generally at very low frequency *in vivo* and *in vitro* (*29, 30, 59*).

In conclusion, hypoxia, which has been shown to protect cancer cells, was also reported to activate the ATR/Chk1 pathway to increase cell survival and protection against ROS mediated DNA damage (*60, 61*). DMC, which has been shown to have increased DNA adduct formation under hypoxic conditions (*29*), can possibly have therapeutic use due to the ability of its adducts to signal for rapid Chk1 degradation, thereby counteracting the cancer-protective effects of hypoxia and should be considered for further investigation into its clinical relevance as a chemotherapeutic.

References

(1) Hollstein, M., Sidransky, D., Vogelstein, B., and Harris, C. C. (1991) p53 mutations in human cancers. *Science 253*, 49–53.

(2) Hollstein, M., Hergenhahn, M., Yang, Q., Bartsch, H., Wang, Z. Q., and Hainaut, P. (1999) New approaches to understanding p53 gene tumor mutation spectra. *Mutat. Res. 431*, 199–209.

(3) Harris, S. L., and Levine, A. J. (2005) The p53 pathway: positive and negative feedback loops. *Oncogene 24*, 2899–2908.

(4) Levine, A. J., Hu, W., and Feng, Z. (2006) The P53 pathway: what questions remain to be explored? *Cell. Death Differ. 13*, 1027–1036.

(5) Johnstone, R. W., Ruefli, A. A., and Lowe, S. W. (2002) Apoptosis: a link between cancer genetics and chemotherapy. *Cell 108*, 153–164.

(6) Deng, C., Zhang, P., Harper, J. W., Elledge, S. J., and Leder, P. (1995) Mice lacking p21CIP1/WAF1 undergo normal development, but are defective in G1 checkpoint control. *Cell 82*, 675–684.

(7) Waldman, T., Kinzler, K. W., and Vogelstein, B. (1995) p21 is necessary for the p53-mediated G1 arrest in human cancer cells. *Cancer Res. 55*, 5187–5190.

(8) Russell, K. J., Wiens, L. W., Demers, G. W., Galloway, D. A., Plon, S. E., and Groudine, M. (1995) Abrogation of the G2 checkpoint results in differential radiosensitization of G1 checkpoint-deficient and G1 checkpoint-competent cells. *Cancer Res. 55*, 1639–1642.

(9) Enders, G. H. (2008) Expanded roles for Chk1 in genome maintenance. *J. Biol. Chem. 283*, 17749–17752.

(10) Osborn, A. J., Elledge, S. J., and Zou, L. (2002) Checking on the fork: the DNA-replication stress-response pathway. *Trends Cell Biol. 12*, 509–516.

(11) Zou, L., and Elledge, S. J. (2003) Sensing DNA damage through ATRIP recognition of RPA-ssDNA complexes. *Science 300*, 1542–1548.

(12) Zhang, Y. W., Otterness, D. M., Chiang, G. G., Xie, W., Liu, Y. C., Mercurio, F., and Abraham, R. T. (2005) Genotoxic stress targets human Chk1 for degradation by the ubiquitin-proteasome pathway. *Mol. Cell 19*, 607–618.

(13) Zhao, H., and Piwnica-Worms, H. (2001) ATR-mediated checkpoint pathways regulate phosphorylation and activation of human Chk1. *Mol. Cell. Biol. 21*, 4129–4139.

(14) Zhang, Y. W., Hunter, T., and Abraham, R. T. (2006) Turning the replication checkpoint on and off. *Cell Cycle 5*, 125–128.

(15) Shen, X., Do, H., Li, Y., Chung, W. H., Tomasz, M., de Winter, J. P., Xia, B., Elledge, S. J., Wang, W., and Li, L. (2009) Recruitment of fanconi anemia and breast cancer proteins to DNA damage sites is differentially governed by replication. *Mol. Cell 35*, 716–723.

(16) Ben-Yehoyada, M., Wang, L. C., Kozekov, I. D., Rizzo, C. J., Gottesman, M. E., and Gautier, J. (2009) Checkpoint signaling from a single DNA interstrand crosslink. *Mol. Cell 35*, 704–715.

(17) Collis, S. J., Ciccia, A., Deans, A. J., Horejsi, Z., Martin, J. S., Maslen, S. L., Skehel, J. M., Elledge, S. J., West, S. C., and Boulton, S. J. (2008) FANCM and FAAP24 function in ATR-mediated checkpoint signaling independently of the Fanconi anemia core complex. *Mol. Cell 32*, 313–324.

(18) Castedo, M., Perfettini, J. L., Roumier, T., Andreau, K., Medema, R., and Kroemer, G. (2004) Cell death by mitotic catastrophe: a molecular definition. *Oncogene 23*, 2825–2837.

(19) Syljuasen, R. G., Sorensen, C. S., Nylandsted, J., Lukas, C., Lukas, J., and Bartek, J. (2004) Inhibition of Chk1 by CEP-3891 accelerates mitotic nuclear fragmentation in response to ionizing Radiation. *Cancer Res. 64*, 9035–9040.

(20) Huang, X., Tran, T., Zhang, L., Hatcher, R., and Zhang, P. (2005) DNA damage-induced mitotic catastrophe is mediated by the Chk1-dependent mitotic exit DNA damage checkpoint. *Proc. Natl. Acad. Sci. U.S.A. 102*, 1065–1070.

(21) Kawabe, T. (2004) G2 checkpoint abrogators as anticancer drugs. *Mol. Cancer Ther. 3*, 513–519.

(22) Dixon, H., and Norbury, C. J. (2002) Therapeutic exploitation of checkpoint defects in cancer cells lacking p53 function. *Cell Cycle 1*, 362–368.

(23) Mukhopadhyay, U. K., Senderowicz, A. M., and Ferbeyre, G. (2005) RNA silencing of checkpoint regulators sensitizes p53-defective prostate cancer cells to chemotherapy while sparing normal cells. *Cancer Res. 65*, 2872–2881.

(24) Didier, C., Cavelier, C., Quaranta, M., Galcera, M. O., Demur, C., Laurent, G., Manenti, S., and Ducommun, B. (2008) G2/M checkpoint stringency is a key parameter in the sensitivity of AML cells to genotoxic stress. *Oncogene 27*, 3811–3820.

(25) Kennedy, K. A., Teicher, B. A., Rockwell, S., and Sartorelli, A. C. (1980) The hypoxic tumor cell: a target for selective cancer chemotherapy. *Biochem. Pharmacol. 29*, 1–8.

(26) Tomasz, M., and Lipman, R. (1981) Reductive metabolism and alkylating activity of mitomycin C induced by rat liver microsomes. *Biochemistry 20*, 5056–5061.

(27) Rockwell, S., Kennedy, K. A., and Sartorelli, A. C. (1982) Mitomycin-C as a prototype bioreductive alkylating agent: in vitro studies of metabolism and cytotoxicity. *Int. J. Radiat. Oncol. Biol. Phys. 8*, 753–755.

(28) Tomasz, M., and Palom, Y. (1997) The mitomycin bioreductive antitumor agents: cross-linking and alkylation of DNA as the molecular basis of their activity. *Pharmacol. Ther. 76*, 73–87.

(29) Palom, Y., Suresh Kumar, G., Tang, L. Q., Paz, M. M., Musser, S. M., Rockwell, S., and Tomasz, M. (2002) Relative toxicities of DNA cross-links and monoadducts: new insights from studies of decarbamoyl mitomycin C and mitomycin C. *Chem. Res. Toxicol. 15*, 1398–1406.

(30) Paz, M. M., Ladwa, S., Champeil, E., Liu, Y., Rockwell, S., Boamah, E. K., Bargonetti, J., Callahan, J., Roach, J., and Tomasz, M. (2008) Mapping DNA adducts of mitomycin C and decarbamoyl mitomycin C in cell lines using liquid chromatography/electrospray tandem mass spectrometry. *Chem. Res. Toxicol. 21*, 2370–2378.

(31) Iyer, V. N., and Szybalski, W. (1963) A Molecular Mechanism of Mitomycin Action: Linking of Complementary DNA Strands. *Proc. Natl. Acad. Sci. U.S.A. 50*, 355–362.

(32) Dronkert, M. L., and Kanaar, R. (2001) Repair of DNA interstrand cross-links. *Mutat. Res. 486*, 217–247.

(33) Boamah, E. K., White, D. E., Talbott, K. E., Arva, N. C., Berman, D., Tomasz, M., and Bargonetti, J. (2007) Mitomycin-DNA adducts induce p53-dependent and p53-independent cell death pathways. *ACS Chem. Biol. 2*, 399–407.

(34) Abbas, T., Olivier, M., Lopez, J., Houser, S., Xiao, G., Suresh Kumar, G., Tomasz, M., and Bargonetti, J. (2002) Differential activation of p53 by the various adducts of mitomycin C. *J. Biol. Chem. 277*, 40513–40519.

(35) Kinoshita, S., Uzu, K., Nakano, K., and Takahashi, T. (1971) Mitomycin derivatives. 2. Derivatives of decarbamoylmitosane and decarbamoylmitosene. *J. Med. Chem. 14*, 109–112.

(36) Yu, J., Zhang, L., Hwang, P. M., Rago, C., Kinzler, K. W., and Vogelstein, B. (1999) Identification and classification of p53-regulated genes. *Proc. Natl. Acad. Sci. U.S.A. 96*, 14517–14522.

(37) Van Houten, B., Cheng, S., and Chen, Y. (2000) Measuring gene-specific nucleotide excision repair in human cells using quantitative amplification of long targets from nanogram quantities of DNA. *Mutat. Res. 460*, 81–94.

(38) Santos, J. H., Meyer, J. N., Mandavilli, B. S., and Van Houten, B. (2006) Quantitative PCR-based measurement of nuclear and mito-chondrial DNA damage and repair in mammalian cells. *Methods Mol. Biol. 314*, 183–199.

(39) Ayala-Torres, S., Chen, Y., Svoboda, T., Rosenblatt, J., and Van Houten, B. (2000) Analysis of gene-specific DNA damage and repair using quantitative polymerase chain reaction. *Methods 22*, 135–147.

(40) Bargonetti, J., Reynisdottir, I., Friedman, P. N., and Prives, C. (1992) Site-specific binding of wild-type p53 to cellular DNA is inhibited by SV40 T antigen and mutant p53. *Genes Dev. 6*, 1886–1898.

(41) Bargonetti, J., Manfredi, J. J., Chen, X., Marshak, D. R., and Prives, C. (1993) A proteolytic fragment from the central region of p53 has marked sequence-specific DNA-binding activity when generated from wild-type but not from oncogenic mutant p53 protein. *Genes Dev. 7*, 2565–2574.

(42) Wang, Z., Aris, V. M., Ogburn, K. D., Soteropoulos, P., and Figueiredo-Pereira, M. E. (2006) Prostaglandin J2 alters pro-survival and pro-death gene expression patterns and 26 S proteasome assembly in human neuroblastoma cells. *J. Biol. Chem. 281*, 21377–21386.

(43) Edinger, A. L., and Thompson, C. B. (2004) Death by design: apoptosis, necrosis and autophagy. *Curr. Opin. Cell Biol. 16*, 663–669.

(44) Zhang, Y. W., Brognard, J., Coughlin, C., You, Z., Dolled-Filhart, M., Aslanian, A., Manning, G., Abraham, R. T., and Hunter, T. (2009) The F box protein Fbx6 regulates Chk1 stability and cellular sensitivity to replication stress. *Mol. Cell 35*, 442–453.

(45) Carrassa, L., Broggini, M., Erba, E., and Damia, G. (2004) Chk1, but not Chk2, is involved in the cellular response to DNA damaging agents: differential activity in cells expressing or not p53. *Cell Cycle 3*, 1177–1181.

(46) Chan, T. A., Hermeking, H., Lengauer, C., Kinzler, K. W., and Vogelstein, B. (1999) 14−3-3Sigma is required to prevent mitotic catastrophe after DNA damage. *Nature 401*, 616–620.

(47) Sidi, S., Sanda, T., Kennedy, R. D., Hagen, A. T., Jette, C. A., Hoffmans, R., Pascual, J., Imamura, S., Kishi, S., Amatruda, J. F., Kanki, J. P., Green, D. R., D'Andrea, A. A., and Look, A. T. (2008) Chk1 suppresses a caspase-2 apoptotic response to DNA damage that bypasses p53, Bcl-2, and caspase-3. *Cell 133*, 864–877.

(48) Hirose, Y., Berger, M. S., and Pieper, R. O. (2001) Abrogation of the Chk1-mediated G(2) checkpoint pathway potentiates Temozolomide-induced toxicity in a p53-independent manner in human glioblastoma cells. *Cancer Res. 61*, 5843–5849.

(49) Wang, J. L., Wang, X., Wang, H., Iliakis, G., and Wang, Y. (2002) CHK1-regulated S-phase checkpoint response reduces camptothecin cytotoxicity. *Cell Cycle 1*, 267–272.

(50) Cho, S. H., Toouli, C. D., Fujii, G. H., Crain, C., and Parry, D. (2005) Chk1 is essential for tumor cell viability following activation of the replication checkpoint. *Cell Cycle 4*, 131–139.

(51) Myers, K., Gagou, M. E., Zuazua-Villar, P., Rodriguez, R., and Meuth, M. (2009) ATR and Chk1 suppress a caspase-3-dependent apoptotic response following DNA replication stress. *PLoS Genet. 5*, e1000324.

(52) Sugiyama, K., Shimizu, M., Akiyama, T., Tamaoki, T., Yamaguchi, K., Takahashi, R., Eastman, A., and Akinaga, S. (2000) UCN-01 selectively enhances mitomycin C cytotoxicity in p53 defective cells which is mediated through S and/or G(2) checkpoint abrogation. *Int. J. Cancer 85*, 703–709.

(53) Merry, C., Fu, K., Wang, J., Yeh, I. J., and Zhang, Y. (2010) Targeting the checkpoint kinase Chk1 in cancer therapy. *Cell Cycle 9*, 279–283.

(54) Arriola, E. L., Lopez, A. R., and Chresta, C. M. (1999) Differential regulation of p21waf-1/cip-1 and Mdm2 by etoposide: etoposide inhibits the p53-Mdm2 autoregulatory feedback loop. *Oncogene 18*, 1081–1091.

(55) Norman, D., Live, D., Sastry, M., Lipman, R., Hingerty, B. E., Tomasz, M., Broyde, S., and Patel, D. J. (1990) NMR and computational characterization of mitomycin cross-linked to adjacent deoxygua-nosines in the minor groove of the d(T-A-C-G-T-A)•d(T-A-C-G-T-A) duplex. *Biochemistry 29*, 2861–2875.

(56) Tomasz, M., Lipman, R., Chowdary, D., Pawlak, J., Verdine, G. L., and Nakanishi, K. (1987) Isolation and structure of a covalent cross-link adduct between mitomycin C and DNA. *Science 235*, 1204–1208.

(57) Sastry, M., Fiala, R., Lipman, R., Tomasz, M., and Patel, D. J. (1995) Solution structure of the monoalkylated mitomycin C-DNA complex. *J. Mol. Biol. 247*, 338–359.

(58) Geacintov, N. E., Cosman, M., Hingerty, B. E., Amin, S., Broyde, S., and Patel, D. J. (1997) NMR solution structures of stereoisometric covalent polycyclic aromatic carcinogen-DNA adduct: principles, patterns, and diversity. *Chem. Res. Toxicol. 10*, 111–146.

(59) Kumar, S., Lipman, R., and Tomasz, M. (1992) Recognition of specific DNA sequences by mitomycin C for alkylation. *Biochemistry 31*, 1399–1407.

(60) Hammond, E. M., Denko, N. C., Dorie, M. J., Abraham, R. T., and Giaccia, A. J. (2002) Hypoxia links ATR and p53 through replication arrest. *Mol. Cell. Biol. 22*, 1834–1843.

(61) Hammond, E. M., Dorie, M. J., and Giaccia, A. J. (2003) ATR/ATM targets are phosphorylated by ATR in response to hypoxia and ATM in response to reoxygenation. *J. Biol. Chem. 278*, 12207–12213.